

# Occurrence of synoptic flaw leads of sea ice in the Gulf of Finland

Ove Pärn<sup>1</sup> and Jari Haapala<sup>2</sup>

<sup>1</sup> *Marine Systems Institute at Tallinn University of Technology, Akadeemia tee 21, EE-12618 Tallinn, Estonia (kylmleek@gmail.com)*

<sup>2</sup> *Finnish Meteorological Institute, Erik Palménin aukio 1, FI-00560 Helsinki, Finland*

*Received 18 Oct. 2009, accepted 16 June 2010 (Editor in charge of this article: Kai Myrberg)*

Pärn, O. & Haapala, J. 2011: Occurrence of synoptic flaw leads of sea ice in the Gulf of Finland. *Boreal Env. Res.* 16: 71–78.

In spite of their importance to the marine ecosystem and winter navigation, flaw leads have not received much attention. This study presents an analysis of the flaw lead occurrence frequency in the Gulf of Finland. We used ice charts of the Estonian Meteorological and Hydrological Institute covering the years 1971–2007 and the Helsinki multi-category sea-ice model. Flaw leads are formed in the Gulf of Finland almost everywhere along the fast-ice edge when moderate or strong winds are acting, but the winds from W, NW, N and S sectors generate a rather uniform lead pattern, thus facilitating navigation in the ice. On average, flaw leads are most common in the Estonian coastal region where their occurrence is typically 10%–30%. However, during severe winters when northerly winds are more frequent flaw leads are also common in the Finnish coastal region.

## Introduction

On the synoptic scale, sea-ice conditions are variable and rapidly changing. Pack ice can drift over 25 km during a stormy day. In a large restricted basin, such as the Gulf of Finland (GoF), sea-ice drift has large horizontal gradients due to the vicinity of landlocked fast ice, causing sea-ice ridging in the compressive regions and opening of pack ice in the divergent regions. A prominent site-specific feature of this differential ice drift is flaw lead, which is defined as open water between pack ice and fast ice. These weather-dependent, synoptic flaw leads are observed frequently in the GoF and in some cases the open water area can extend over several hundred kilometers.

Generation of flaw leads enhances heat and moisture exchange between the atmosphere and the ocean, leading to increased fogging and pre-

cipitation in the atmosphere and intensified vertical mixing and ventilation in the ocean. It is especially important in the Arctic Ocean in the regions of perennial sea-ice cover, where flaw leads have quite often a large extent and duration (Kassens 1994) and have important consequences for functioning of the marine ecosystem.

In the Arctic, the Laptev Sea is a region where flaw leads are commonly observed. Dynamics of flaw leads were first studied by Zakharov (1966). Later, Dethleff (1994), Dethleff *et al.* (1998) and Liu *et al.* (2009) showed that the Laptev Sea flaw lead is driven by hydrometeorological factors and bathymetry. A very long lead (approximately 2000 km long) lies at up to 30 m water depth, bordering the coastal fast ice. The width of the open water ranges from 100 m to 25 km depending on synoptic winds. The flaw lead favors circulation of deep and near-bottom waters. It has

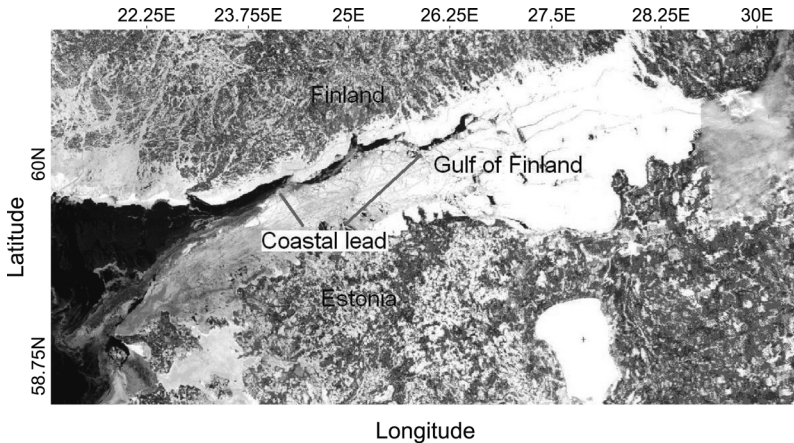


**Fig. 1.** Ice situation in the Gulf of Finland on 20 January 2003 (Moderate Resolution Imaging Spectrometer image by Liis Sipilgas). Observed situation was preceded moderate NW and N winds on 19 and 20 January.

also environmental effects like enhanced sediment transport (Stein and Korotov 1994).

Flaw leads are also natural fairways for vessels navigating in ice (Fig. 1). Although this aspect is not widely explored in scientific literature, in practice seafarers tend to utilize flaw leads whenever possible. In enclosed basins with seasonal ice cover, the shipping aspect of flaw leads in local economy is apparently more important than the impacts of leads on the regional climate are.

The GoF is one of the most intensive shipping regions in the world (Sonninen *et al.* 2006). During the last decade, oil transportation from Russian terminals has increased remarkably, intensifying essentially the tanker traffic along the GoF. This tendency is predicted to continue, and much attention has been paid to navigational safety, especially in winter, both on scientific and management levels (HELCOM 2007).

Under average winter conditions, ships have to navigate in the Baltic Sea at least 150 nautical miles in ice-covered waters, while during a very severe winter, the ice-sailing distance can exceed 400 nautical miles (Seinä and Palosuo 1996). Some ice forms even during mildest winters. The ice season begins usually in December when the shallow coastal regions are frozen in the easternmost GoF. On average, the ice season lasts until the middle of April, but in small bays sea ice remains until May. In winter, sea ice should be considered a primary factor causing ship damages that may result in pollution.

Flaw leads in the Baltic have not yet been studied much. The only published study so far

was conducted by Haas (2004), who carried out detailed ice thickness measurements along the whole Finnish coastline in February 2003 using the helicopter-borne electromagnetic-inductive (HEM) method. The flaw lead detected in the GoF was surrounded by thick deformed ice (up to 5 m) between Helsinki and Tallinn. The flaw leads, detected by the HEM method, were in general well visible also on the routine ice charts.

The objective of this work is to analyze the occurrence frequency of flaw leads in the GoF. We analyze EMHI (Estonian Meteorological and Hydrological Institute) ice charts and utilize the Helsinki multi-category sea-ice model in order to study the appearance of leads and determine how lead formation depends on the large-scale wind direction.

## Material and methods

### Observational data

This study is based on the ice charts covering the period 1971–2007. The ice charts used here were compiled by the EMHI using their own observations as well as the charts of the Finnish Ice Service and the Russian ice charts, which rely largely on satellite data and visual observations from air, land and ships. Every chart represents the ice distribution over the GoF on a particular date.

Here, in surveying and analyzing the ice charts, the flaw lead is defined as a narrow linear

region of open water, new ice or region of low ice concentration that is located either between two areas of compact ice or between pack ice and fast ice.

The ice charts were converted into matrixes for every date (an example matrix for 22 February 1996 is presented in Table 1). The data on the distribution of wind direction in the middle of the GoF (Fig. 2) are based on the NCEP/NCAR reanalysis. In spite of the coarse resolution of the NCEP/NCAR data, they describe average wind conditions in the Baltic Sea area very well: the correlation coefficient between the NCEP/NCAR data and surface observations is 0.91 for zonal and 0.88 for meridional components of the wind (Pärn and Haapala 2007).

**Model experiments**

The HELMI (HELsinki Multicategory Ice model) model used in this study, resolves ice thickness distribution, i.e. ice concentrations of different thickness categories, redistribution of ice categories due to deformations, thermodynamics of sea ice, horizontal components of ice velocity and internal stress of the ice pack. An ice pack is a mixture of open water and undeformed and deformed ice categories of variable thickness. Deformed ice is separated into rafted- and ridged-ice classes. The model has been used in large-scale studies (Haapala *et al.* 2005) and operational applications. The model physics and numerics are the same for both operational and climate simulations. The only differences are in the horizontal resolution and atmospheric data used for calculations of surface heat and momentum fluxes.

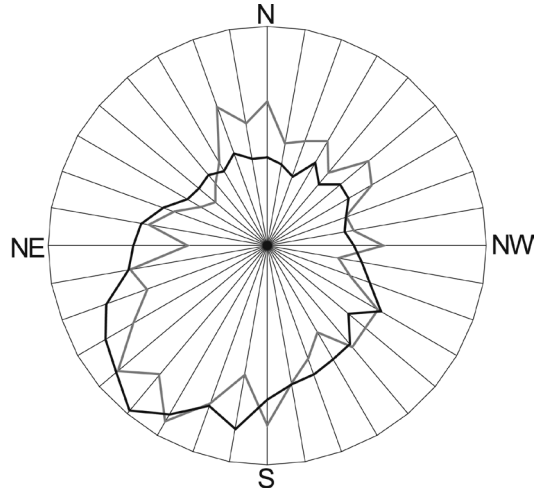


**Fig. 2.** Directional frequency distribution of the winds with daily speed over 4 m s<sup>-1</sup> in winter (January–April). Data from 1971–2007 for the middle of the Gulf of Finland. Black line in the rose indicates average winter and grey line severe winter.

The present setup of the sea-ice model simulated evolution of five undeformed and two deformed ice categories. Ice categories are not restricted to any particular ice thicknesses except for the thinnest ice-thickness category that is not allowed to exceed 10 cm. Deformed ice is divided into two categories: rafted ice and ridged ice. The horizontal resolution of the model is 1 nautical mile.

**Observed ice deformations: leads with respect to navigability**

An example of an individual ice chart, avail-

**Table 1.** Ice chart (Fig. 3) converted into a matrix. 0 stands for ice cover and 1 stands for open water, new ice or a region of a low ice concentration.

	23°–24°E	24°–25°E	25°–26°E	26°–27°	27°–28°E	28°–29°E	29°–30°E
60°30'–60°20'N	0	0	0	0	0	0	0
60°20'–60°10'N	0	0	0	1	0	0	0
60°10'–60°00'N	0	0	1	1	0	0	0
60°00'–59°50'N	0	1	0	0	0	0	0
59°50'–59°40'N	1	0	0	0	0	0	0
59°40'–59°30'N	0	0	0	0	0	0	0
59°30'–59°20'N	0	0	0	0	0	0	0
59°20'–59°10'N	0	0	0	0	0	0	0

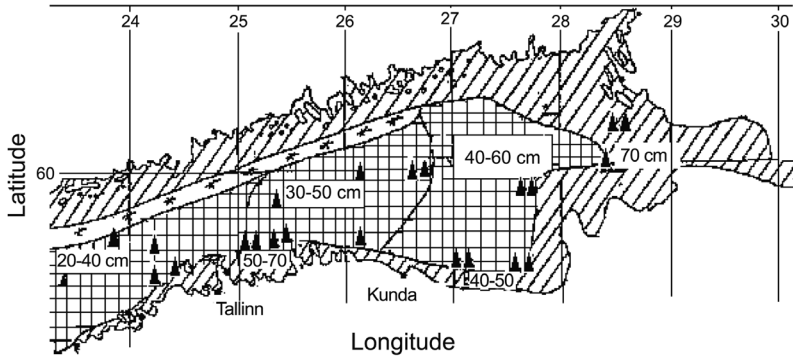


**Fig. 3.** The EMHI ice chart for the date of the largest ice extent (22 February 1996) in the ice season 1995/1996. During the previous few days winds blew alternately from N, NE and NW. The triangles indicate ridged ice, diagonal lines fast ice and squares consolidated ice.

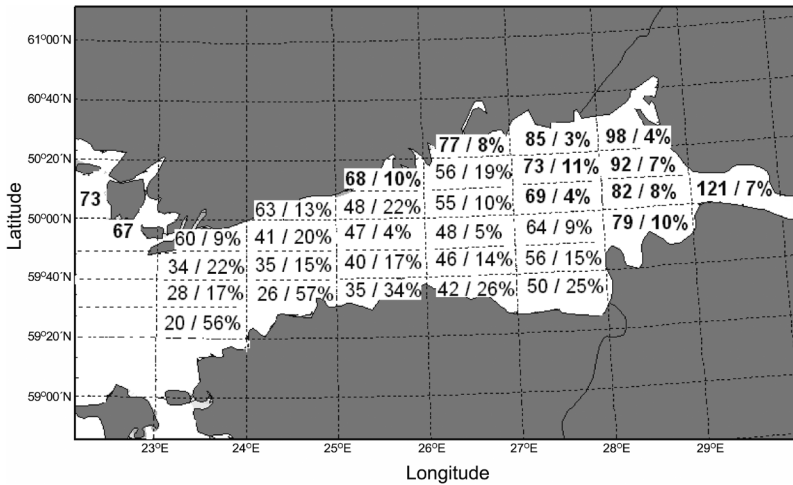


**Fig. 4.** Average ice conditions in the Gulf of Finland during 1971–2007 in the 1.0° long. × 0.2° lat. grid. The first number in the cells is the average duration of the ice cover in days, and the second is the ice lead occurrence expressed as the percentage of the ice days.

able from the EMHI database, is given in Fig. 3. During the maximum ice extent, ridged ice covers large offshore areas of the GoF, and ice thickens towards the east. Ice is ridging more severely in the narrowest part of the GoF between 25°E and 25°30'E and in its widest part between 27°E and 28°E. Also notable differences in ice properties in the north–south direction are evident. As strongest winds blew from NW, N and NE before 22 February — that is prior to the generation of the ice chart (Fig. 3) — ice drifted southwards generating a lead about 10–20 km from the Finnish coast. In the compressive region to the south and east of landfast, ice ridges were formed.

The ice-cover period and the occurrence of leads (percentage of ice days) in different regions of the GoF were calculated from the ice charts covering the period 1971–2007. The statistics was calculated for the regular 1.0° long. × 0.2° lat. grid.

We also examined which areas are favorable for navigation and harbors, assuming a low ice concentration allows flaw leads to favor shipping, whereas the regions of high ice concentration are typically also regions of deformed ice, which are obstacles to navigation.

The occurrence of leads is the most common in the Estonian coastal area, where their occurrence is typically 10%–30% (Fig. 4). In the middle of the GoF, leads make up a much smaller percentage. For example, between 25°E and 26°E, the lead occurrence was only 4% in the middle of the basin, whereas it increased to 22% at the Finnish coast and to 34% at the Estonian coast. The lead occurrence was highest at the entrance to the GoF due to thin ice — a result of a short ice-cover period — as well as ice-cover disturbance caused by winds and sea currents.

In order to find the relationship between the wind direction and the spatial pattern of the lead occurrence, we calculated wind distributions for

days when the daily wind speed exceeded  $4 \text{ m s}^{-1}$  as lower wind speeds are not expected to cause ice drift. The analysis revealed that moderate and strong winds blew mostly from SW. The frequency of winds from the S–W sector was 37%, while those from the opposite sector (between N to E) was only up to 21%.

## Results of the numerical analyses

We estimated how the ice deformation rate and open water formation are related to wind direction and how these vary at a regional scale. The results are based on the idealized numerical analyses, in which sea ice was initially constant: the level ice thickness was set to be 0.35 m, the ice concentration  $A = 0.99$ . Then the response of the sea-ice model to constant,  $10 \text{ m s}^{-1}$  wind from different directions was calculated.

In order to analyze which wind directions facilitate navigation in ice, we assumed that in those regions where the modeled ice concentration was below 85%, the ships could navigate without any difficulties. The grid points with a low ice concentration were considered equivalent to flaw lead areas.

Under northerly winds, an extensive flaw lead, parallel to the coastline, extended from the mouth to the end of the GoF (Figs. 1 and 5a). In that case, vessels could easily navigate in the Finnish coastal zone. However, the picture was quite different under north-easterly winds. This wind situation also generated much open water, but contrary to the previous case, open water areas were separated by an island, and uniform lead was generated only in the easternmost part of the GoF (Figs. 5b and 6). Such a situation was observed on 22 February 1996, when — due to NW, N and NE winds on the previous day — a lead occurred throughout the GoF from the estuary ( $23^\circ\text{E}$ ) to almost the middle of the ventrix ( $27^\circ\text{E}$ ) (Fig. 3).

Also southerly winds, blowing transverse to the basin, were favorable for the flaw lead generation (Fig. 5). In this case, the lead was located by the Estonian coast reaching from the mouth ( $23^\circ\text{E}$ ) to the central part of the GoF ( $28^\circ\text{E}$ ), while a few minor leads did exist by the Ingerian (southern) shore of the GoF (between  $28^\circ\text{E}$

and  $29^\circ\text{E}$ ). The EMHI ice charts for 1971–2007 show that leads appeared quite often near the Estonian coast (Fig. 4). Thus the model results reflect well the empiric data.

Southwesterly winds were the most common in winter (Fig. 2). In those cases, a minor lead was formed near the Estonian coast in the middle of the GoF (Fig. 5f).

During flaw-lead formation events, sea ice was ridging and thickening in some regions of the GoF. To estimate the mean thickness of deformed ice, the thickness was integrated over the latitude  $L$  ( $59^\circ25'\text{N}$ – $60^\circ30'\text{N}$ ). The latitude-integrated deformed ice thickness is

$$H = \frac{1}{L} \int_{L_1}^{L_2} \tilde{h} dL,$$

where  $\tilde{h}$  is the mean deformed ice thickness in the model grid (Haapala *et al.* 2005). Figure 7 presents how the mean deformed ice thickness varied in space and is thickening in time under an action of the SW wind. After five hours of the SW wind action, the deformed ice grew over 0.01 m thicker at the longitudes  $24^\circ30'$ ,  $25^\circ30'$ ,  $27^\circ$ ,  $28^\circ$ ,  $28^\circ30'\text{E}$ . Further, we can see that deformed ice grew 0.07–0.1 m thicker per day in those regions, whereas between these areas the deformed ice grew less than 0.01 m during the same time.

## Discussion and conclusions

The presence of sea ice in the GoF for 3–5 months each winter is a challenge for winter navigation. Flaw leads, as natural waterways, can greatly facilitate shipping. In this work, we examined the frequency of flaw leads based on daily ice charts and modeled ice conditions to study how lead formation depends on wind.

Flaw leads are a common feature in the GoF. Practically winds from all directions generate open water and leads in pack ice, but winds from W, NW, N and S in particular form a rather uniform lead pattern thus facilitating navigation in the ice (Fig. 8). This is important during severe winters when the GoF is fully covered by thick and ridged ice.

On average, flaw leads were the most common in the Estonian coastal region. How-

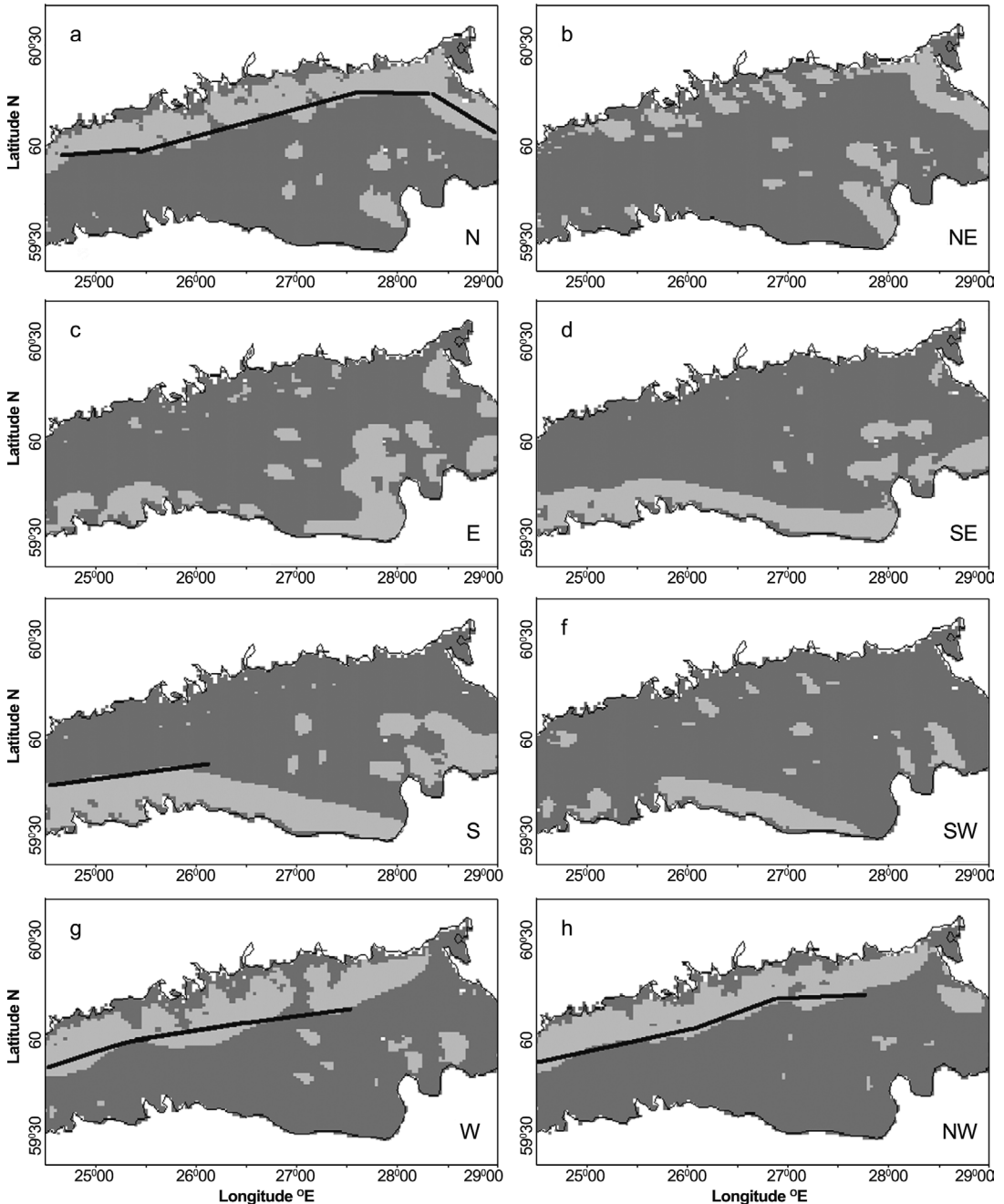


**Fig. 5.** The modeled occurrence of leads during different wind conditions in the Gulf of Finland. Light grey indicates the lead and dark grey indicates an area fully covered by ice. The line shows an optimal route of a vessel navigating in ice.

ever, during severe winters, northerly winds were more frequent and therefore also flaw leads were common in the Finnish coastal region. Under certain conditions, the same dominant wind direction could prevail for several weeks,

leading to a situation that flaw lead is extended as far as the middle of the basin.

Concurrent with generation of flaw leads, drift ice is also compacting and ridging in the opposite side of the basin. In order to show how

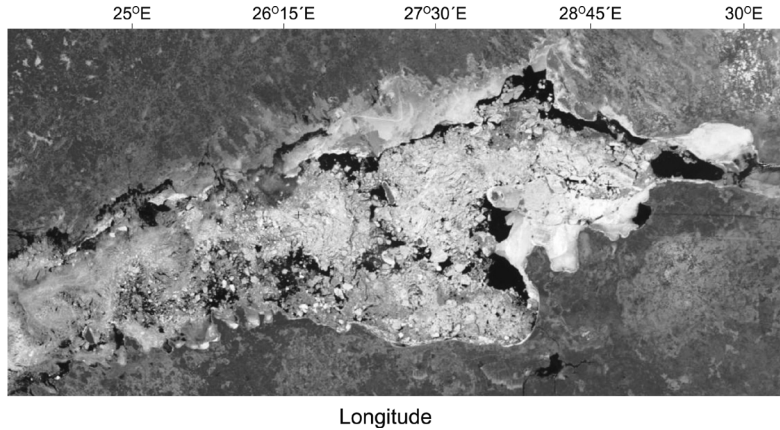


**Fig. 6.** Ice situation on 20 April 2003. On 19 and 20, April the wind blew from NNE and N with speeds of 0–2 m s<sup>-1</sup>, on 18 April the speed of the NE wind was 4–8 m s<sup>-1</sup>. Consequently, generated ice-free regions are patchy.

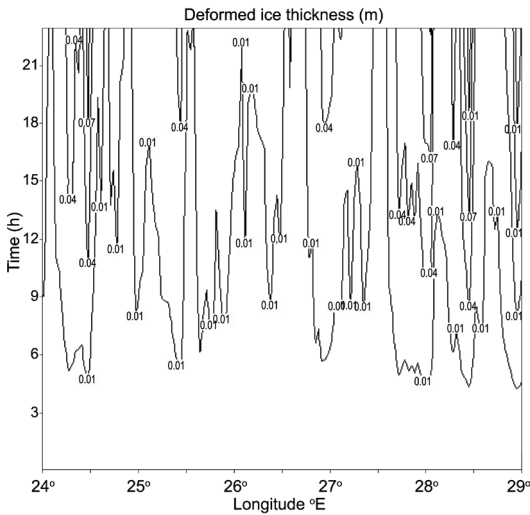


**Fig. 7.** The mean thickness of deformed ice as a function of longitude and time after the onset of constant SW wind of 10 m s<sup>-1</sup>, starting from the horizontally homogeneous ice conditions.

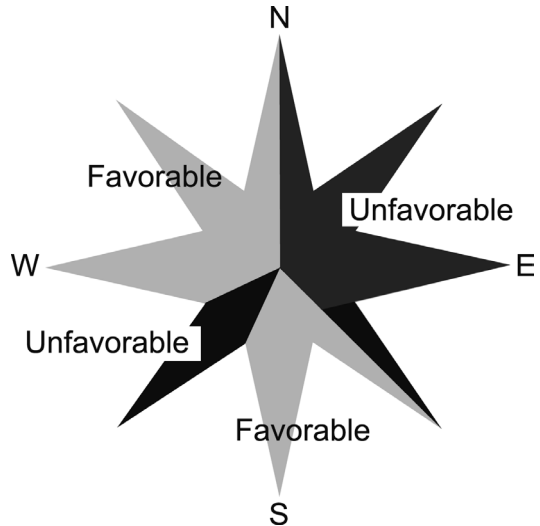


**Fig. 8.** Ice conditions favoring vessel navigation form along the Gulf of Finland when a constant wind blows for at least 10 h. W, NW, N and S winds generate a rather uniform lead pattern, thus facilitating navigation in the ice.

important the mechanical thickening of ice is, we can compare growth rates the deformed ice with the thermodynamic growth rate of ice. If the air temperature is -10 °C, then 0.35-m thick ice grows by about 0.01 m per day. Thus the thermodynamic growth rate of undeformed ice is slow as compared with that of the deformed ice since in the same conditions, the new ice in the leads is thickening by about 0.05 m per day.

The ship damage risk is higher closer to the areas of high ice deformation rate where ice floes of different properties meet, yielding also a clear ice thickness gradient (Pärn *et al.* 2007). Such

situations occur when navigating from an area of low-concentrated ice to an area of high-concentrated thick, probably ridged ice. The present study enables for a rough estimate of the navigation conditions based on the weather forecast and gives a few general guidelines for selecting the routes under severe ice conditions.

*Acknowledgments:* This study was supported by the Estonian Science Foundation (grant no. 7328). We wish to thank the Estonian Meteorological and Hydrological Institute (Kai Loitjäär, Riina Vahter) and Liis Sipelgas, who shared with us SAT images.

## References

- Dethleff D. 1994. Dynamics of the Laptev Sea flaw lead. *Ber. Polarforsch.* 144: 49–54.
- Dethleff D., Loewe P. & Kleine E. 1998. The Laptev Sea flaw lead — detailed investigation on ice formation and export during 1991/1992 winter season. *Cold Reg. Sci. Technol.* 27: 225–243.
- Haapala J., Lönnroth N. & Stössel A. 2005. A numerical study of open water formation in sea ice. *J. Geophys. Res.* 110: C09011.1–C09011.17.
- Haas C. 2004. Airborne EM sea-ice thickness profiling over brackish Baltic Sea water. In: *17th International Symposium on Ice, International Association of Hydraulic Engineering and Research*, Saint Petersburg, pp. 12–17.
- HELCOM 2007. Towards a Baltic Sea with environmentally friendly maritime activities. In: *2nd Stakeholder Conference on the HELCOM Baltic Sea Action Plan*, Helsinki, pp. 5–25.
- Kassens H. & Thiede J. 1994. Climatological significance of Arctic sea ice at present and in the past. *Ber. Polarforsch.* 144: 81–86.
- Liu C., Chang Y.-C., Huang S., Yan S.-Y., Wu F., Wu A.-M., Kato S. & Yamaguchi Y. 2009. Monitoring the dynamics of ice shelf margins in Polar Regions with high-spatial- and high-temporal-resolution space-borne optical imagery. *Cold Reg. Sci. and Technol.* 55: 14–22.
- Pärn O. & Haapala J. 2007. Analysis of the ice model simulation for the Gulf of Finland in 2002/03. *Ber. Bundesamt. Seesch. Hydrogr.* 42: 37–45.
- Pärn O., Haapala J., Kõuts T., Elken J. & Riska K. 2007. On the relationship between sea ice deformation and ship damages in the Gulf of Finland in winter 2003. *Proc. Estonian Acad. Sci. Eng.* 13: 201–214.
- Seinä A. & Palosuo E. 1996. The classification of the maximum annual extent of ice cover in the Baltic Sea 1720–1995. *Meri* 27: 79–91.
- Sonninen S., Nuutinen M. & Rosqvist T. 2006. Development process of the Gulf of Finland Mandatory Ship Reporting System. *VTT Publ.* Espoo, pp. 12–30.
- Stein R. & Korolev S. 1994. Shelf-to-basin sediment transport in the eastern Arctic Ocean. Russian–German cooperation in the Siberian shelf seas: geo-system Laptev–Sea *Ber. Polarforsch.* 144: 87–100.
- Zakharov V.F. 1966. The role of flaw leads off the edge of fast ice in the hydrological and ice regime of the Laptev Sea. *Acad. Sci. USSR* 6: 815–821.